Emissions from Fires Consequences for Human Safety and the Environment

Blomqvist, Per

2005

Modelling of hydrogen cyanide formation in room fires

Tuovinen H., Blomqvist P. and Saric F.

Fire Safety Journal 39 (2004) 737-755

Paper VIII

Available online at www.sciencedirect.com
SCIENCE DIRECT®
Fire Safety Journal 39 (2004) 737–755
FIRE SAFETY JOURNAL
www.elsevier.com/locate/firesaf

Modelling of hydrogen cyanide formation in room fires

Heimo Tuovinen[a,*], Per Blomqvist[a], Fikret Saric[b]

[a]*SP Swedish National Testing and Research Institute, Fire Technology, P.O. Box 857, S-501 15 Borås, Sweden*

[b]*Division of Combustion Physics, Lund Institute of Technology, P.O. Box 118, S-221 00 Lund, Sweden*

Received 26 November 2003; received in revised form 2 June 2004; accepted 22 July 2004
Available online 16 September 2004

Abstract

A chemical kinetics model for calculation of the formation of hydrogen cyanide (HCN) has been made. The combustion of a mixture of methylamine and ethylene has been modelled using the stationary laminar flamelet concept. The flamelet calculations are based on several thousand elementary reaction steps including the chemical kinetics of HCN in combustion. The flamelets for both cold (293 K) and hot (1000 K) combustion product recycling have been calculated. The effect of strain is also included in the flamelet calculations. Scalar dissipation rates from $0.01\,s^{-1}$ to extinction values have been varied. Also the effect of radiation is included in the flamelet state relationships.

Separate flamelet sets for various levels of radiation, from adiabatic up to 30% radiation losses, incremented by 1%, have been made. In the flow field calculation, the flamelet options may be used either as adiabatic, constant radiation or an interpolation between flamelet sets of different radiation.

The chemical kinetics model, incorporated into a Reynolds-Averaging Navier–Stoke (RANS) type CFD code, has been used to simulate two laboratory fire tests of the combustion of nylon. Changing the size of the opening in the test room varied the ventilation between the two tests. Flamelet sets for a mixture of methylamine and ethylene with nitrogen content close to that of nylon were used in these simulations. The simulations were made with and without recycling the combustion products back to the fire.

The calculations show that recycling of the combustion products to the fire increases the formation of HCN and CO. Similarly, a lowered ventilation rate increases the formation of

*Corresponding author. Tel.: +46-33-165567; fax: +46-33-417759.
E-mail address: heimo.tuovinen@sp.se (H. Tuovinen).

doi:10.1016/j.firesaf.2004.07.003

these species. The calculated temperatures and main species concentrations, including HCN, agree reasonably well with the trends in the laboratory measurements.

Keywords: Flamelet models; CFD models; Hydrogen cyanide; Vitiation; Under-ventilated fires

1. Introduction

Hydrogen cyanide (HCN) can be formed in combustion of any nitrogen-containing material. HCN is about 35 times more toxic than carbon monoxide (CO). Further the influence of HCN on humans is quite different to that of CO. HCN is carried rapidly to the brain by the blood, making the victim quickly incapacitated. The uptake rate is directly related to the concentration of HCN in the air the victim is breathing. As low as 20 ppm, HCN in the air shows symptoms in victims after extended exposure times, concentrations of 120–150 ppm may be life-threatening after a half an hour, and a concentration of 3000 ppm (0.3% by volume) may directly lead to death. Because of its high toxicity HCN is important in designing the evacuation routes from fires. A more detailed description of the effects of HCN on humans is presented in Ref. [1].

The interest in studies of the nitrogen chemistry in combustion has arisen from the need to understand the mechanisms behind NO_X formation. Earlier research by Fenimore [2] indicated that the conversion of organic nitrogen compounds to NO_X was nearly independent of the parent molecule, and that local combustion conditions and the initial concentration of the nitrogen species were the dominant factors. Fenimore further speculated that an intermediate product was formed that could react to either NO or N_2 depending on the combustion conditions. Bowman [3] later proposed that for simple nitrogen-containing fuels, a reasonable prediction of NO_X formation could be achieved by using a global reaction step of fuel-nitrogen → HCN combined with detailed HCN chemistry [4].

In investigations of the production and dispersion of HCN with fire-induced flows in multi-room buildings, CFD has the potential to be a valuable tool. Large-scale fire tests are very expensive and it is practically impossible to make detailed measurements of HCN in as many points as necessary to estimate the true dispersion pattern.

In order to model a fuel using CFD, its combustion characteristics must be well known. Further, the combustion of the fuel should be easy to control and vary. To have such properties, the fuel should be in the gas phase. It is difficult, however, to find a nitrogen-containing fuel, relevant from a fire safety point of view, that is in gas phase at room temperature. Therefore, a fictitious mixture of two fuels, ethylene and methylamine, was chosen as a generic model fuel for the CFD simulations presented in this paper. A chemical kinetic model was incorporated in the stationary laminar flamelet concept, which described the combustion of the fuel. The burning of nylon in a room configuration was simulated as a first trial, using the model fuel (i.e. a mixture of ethylene and methylamine) with a content of nitrogen as that of nylon.

To quantitatively compare the results regarding HCN of the experiments with those of the simulation, one has to make the presumption that the pyrolysis chemistry of nylon gives the same types and proportions of nitrogen-containing breakdown products as those described by the reaction mechanism for methylamine incorporated in the model. Such a presumption would perhaps not be entirely true, but based on the more qualitative knowledge discussed above that "the conversion of organic nitrogen compounds to NO_X (where HCN is the major intermediate product) is nearly independent of the parent molecule" semi-quantitative results with some significance should be attainable with the proposed approach.

Emission of HCN from combustion of common materials used in our home environment has been presented previously [1]. The materials chosen were: synthetic rubber, nylon, wool, polyurethane and melamine. All the materials were tested in small scale with varying degrees of ventilation in both flaming and non-flaming conditions. These tests showed that HCN was produced from all the materials, particularly from non-flaming combustion and under conditions of restricted oxygen availability.

In room fires, the oxygen content in the air that is entrained into the fire is usually lower than in fresh air. The air in the fire location usually also contains the products of combustion, i.e., the air is vitiated. This reduces the combustion efficiency and yields more products of incomplete combustion. Thus, to model the chemistry correctly, the boundary conditions for flamelets must be modified to take the effect of vitiation on the chemistry into account. As the re-circulation varies as the fire grows so does the contents of combustion products in the air. There is, therefore, a need to calculate the flamelets for varying degrees of vitiation. Depending on the ventilation conditions, fire size compared to room size and other burning conditions, the recycled combustion products may be either hot or cold [5]. Therefore the flamelets should also be calculated using boundary conditions on the oxidant side for both cold and hot vitiation. Flamelets calculated for a vitiated atmosphere have not been commonly used to date. The first work of calculated flamelets for vitiated air was made in 1991 [5–7], prior to the connection of the flamelet model to CFD.

The work presented in this paper takes the formation of hydrogen cyanide into account [8]. The chemical kinetic model used in the calculations consists of several thousand chemical reactions including the kinetics of hydrocarbons (C_1–C_4) [9] and NO_X species [10,11]. The flamelet calculations carried out in this study used the so-called 'Arc Length Continuation Method' [12], which solves a set of differential equations, including the inverse of scalar dissipation rate as a variable. The methylamine oxidation mechanism used in this study as a sub-scheme consists of 350 elementary reaction steps according to Kantak et al. [13], including H-atom abstraction, C–N bond scission, formation of HCN and NH_3 and recombination reactions of H_2CN and CH_3NH. Pathways leading to formation of HCN are usually preceded by H-abstractions starting from methylamine (CH_3NH_2):

$$CH_3NH_2 \rightarrow \text{intermediate} \rightarrow \text{smaller intermediate} \rightarrow HCN$$

The products after C–N bond scission reactions in the fuel molecule usually play a minor role in the formation of HCN.

The increase of the chemical reaction scheme demands an increase in computer storage and computing time, of which the computing time is the limiting factor. Thus, the chemistry calculations are not convenient to perform at the same time as the flow-field calculations. Even though we have relatively fast computers today, the calculation of the chemistry at every node (control volume) at each time step, would be unrealistically time consuming. In this work, the chemical kinetic calculations were removed from the flow-field calculations due to the huge chemical reaction scheme involved and the need to calculate these under varying physical conditions, such as vitiation. Instead, pre-calculated flamelet state relationships were stored in so-called flamelet libraries for use in flow-field calculations with CFD.

2. Calculated flamelets

The flamelets are calculated for the combustion of the model fuel (i.e. a mixture of methylamine and ethylene) in pure air and are additionally calculated for the fuel mixture in air including the main combustion products (H_2O and CO_2), i.e. the effects of vitiation are included in the flamelet library. Further, the effects of radiation and strain rate are included (see below). The fuel mixture was designed to have a nitrogen content of 12.2% by weight, in order to facilitate simulation of e.g. the combustion of nylon-6,6. This gave a proportion of 1:3 for methylamine to ethylene in the fuel mixture. A flamelet library of a fuel mixture with a lower nitrogen content (3.8% by weight, 1:12 proportions of methylamine and ethylene) was additionally calculated. This fuel is not included in the simulations reported on in this article, but will be an important tool in further studies of combustion of nitrogen-containing fuels.

2.1. The flamelet library

The flamelets for HCN-generating fuels have been added to the existing flamelet library in the Reynolds-Averaging Navier–Stoke (RANS) type CFD code: SOFIE [14]. The number of flamelet sets in this new flamelet library is very large. The flamelets are calculated for a non-vitiated oxidiser stream and for eight levels of both cold and hot vitiation in the oxidiser stream, for two mixtures of fuel, i.e. a total of 34 configurations. Each of these configurations includes a separate sub-library of flamelets. Further, each sub-library consists of flamelets with about 30 different values of strain rate (scalar dissipation) and, for every strain rate, 30 sets of flamelets for varying radiation. Thus, the total number of flamelet sets is more than 30,000. A schematic block scheme of the current version of the flamelet model for use in SOFIE is shown schematically in Fig. 1.

The flamelet lookup tables are pre-computed from the instantaneous state relationships by integrating for each property throughout the mixture fraction and mixture fraction variance space. The mixture fraction mean has been discretised in

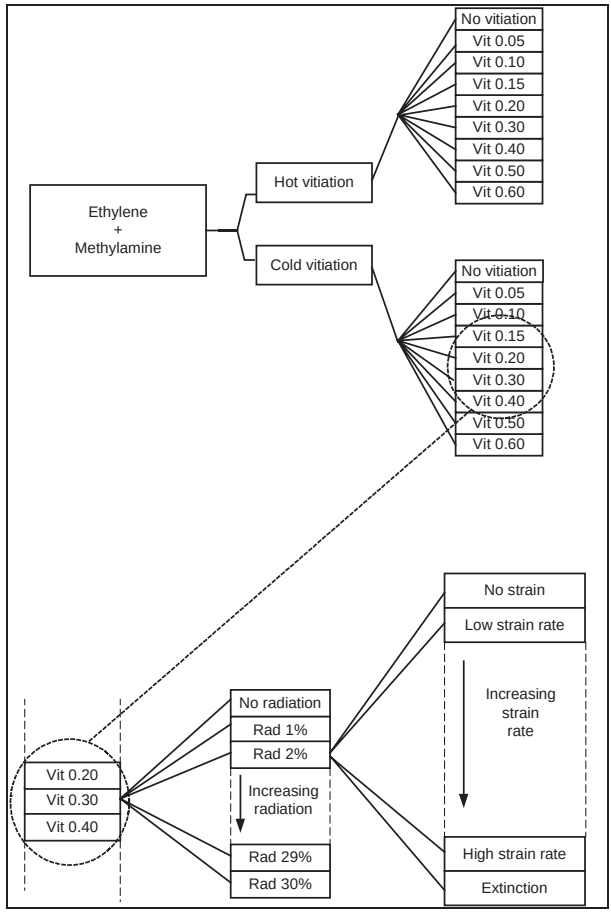

Fig. 1. Flamelet library structure for vitiated and non-vitiated air used in SOFIE. For each vitiation fraction there are 30 different sets of flamelets for each radiation increment and for each radiation level there are about 30 individual sets of flamelets for varying strain rate.

101 divisions, and the mixture fraction variance in 51 divisions. The minimum and maximum values of mixture fraction variance of 0.001 and 0.1, respectively, have been employed. As the turbulence intensity of fires in atmospheric conditions is relatively low compared with other combustion processes such as internal combustion engines, normally only low strain rates, 0.04–0.08 s^{-1}, are taken into account. The flamelets are, however, calculated up to extinction values of strain rate. When simulating fire with very high turbulent intensity, the flamelets for higher strain rate should be selected in the calculations.

This model is still run with single values for vitiation and strain rate in the whole calculation domain at any given time, and not with individual values of these

parameters for each control volume. Allowing the use of a unique description of these parameters in each control volume would require two additional dimensions in the lookup table, which would require much more computer storage and correspondingly greater computation times. For the calculation of radiative losses, however, there are options included for running with fixed values, or alternatively with varying values (see Section 2.3) based upon the local heat loss with respect to adiabatic conditions.

2.2. Effect of vitiation

The flamelets are calculated for various degrees of vitiation, i.e. fire gas re-circulation, which means that the oxidiser stream is mixed with a fraction of re-circulated combustion products. Only the products of complete combustion (H_2O and CO_2) are re-circulated. Flamelets with vitiation fraction from zero to 0.60 were calculated, at increments of 0.05 up to 0.20 vitiation and 0.10 for higher levels of vitiation. Further, the flamelet sets for both cold and hot vitiation are included. For cold vitiation the temperatures of both fuel and air streams are held at 293 K. For hot vitiation the fire gases are assumed to have a temperature of 1000 K. The temperature of the vitiated air is calculated as the arithmetic mean of the hot gas at 1000 K and air at 293 K (equal heat capacities for hot gas and air assumed). Thus, the temperature of the oxidiser stream is a linear function of vitiation fraction.

Species concentrations in the oxidiser stream vary with vitiation. Increased vitiation affects the chemistry, reducing the combustion efficiency, which leads to the generation of more products of incomplete combustion such as CO and HCN. The mole fractions of species in the oxidiser stream for the fuel mixture as a function of the vitiation fraction are shown in Fig. 2.

Figs. 3(a–d) and 4(a, b) show selected flamelet profiles as calculated from the chemical kinetic model, where species concentrations and temperature are expressed as a function of the mixture fraction. In these figures, the effects of vitiation can be seen.

In the simulations presented in this article only the cold vitiation option was used. Thus, the flamelet profiles in Figs. 3 and 4 show data of cold vitiation only. Further, effects of heat losses due to radiation have been omitted in these figures. It is evident from Fig. 3(b) that the adiabatic combustion temperature is reduced during vitiated conditions and that the production of HCN (Fig. 3(a)) generally, over the entire mixture-fraction range, is likewise reduced. It is, however, somewhat misleading to take the full mixture fraction range into account when interpreting the flamelet profiles for the products from combustion. Actually, the greatest part of the combustion takes place in a narrow mixture-fraction range around stoichiometric conditions and extinction occurs under fuel-rich conditions (generally at a mixture fraction of 0.2–0.3).

In Figs. 3(c) and (d) the interesting mixture-fraction range has been enlarged. For the non-vitiated case it can be seen that HCN is not produced at stoichiometric conditions; only a fuel-rich mixture would yield HCN in this case. However, with an increased vitiation the combustion temperature is decreased and HCN is produced at

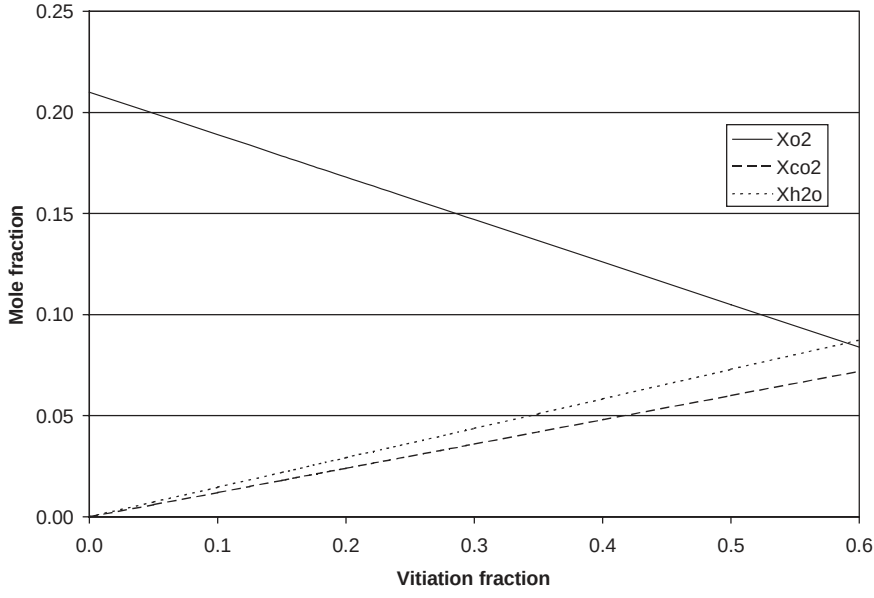

Fig. 2. The mole fractions of oxygen and main combustion products as a function of vitiation fraction in the oxidiser stream.

considerably lower values of mixture fraction. Note that the value representing stoichiometric conditions (mixture fraction = 0.0693) in Fig. 3(c, d) is calculated for the non-vitiated case, and will hereafter be referred to as 'nominal stoichiometric conditions'. In the vitiated case, however, combustion gases lower the oxygen concentration in the oxidiser stream and the effective stoichiometric mixture fraction would thus, in this case, be shifted to a lower value.

The flamelet profiles of CO and CO_2 are shown in Figs. 4(a) and (b), respectively. For CO, it can be seen that the production is generally enhanced with a moderately increased vitiation, for values of the mixture fraction in the region of, and below, nominal stoichiometric conditions. Actually, contrary to HCN, CO is produced even for a fuel-lean mixture at non-vitiated conditions. The mole fraction of CO_2 peaks close to stoichiometric conditions for the non-vitiated case, as the most efficient combustion takes place here. The mole fraction generally increases with vitiation in spite of the poorer combustion, but this is due to the fact that CO_2 is a major part of the recirculated combustion gas in the vitiated cases. However, in the region of nominal stoichiometric conditions, it is clear that a moderate vitiation lowers the mole fraction of CO_2.

2.3. *Effect of radiation*

Separate flamelet sets for various levels of radiation, from adiabatic up to 30% radiation losses, incremented by 1%, have been made. In the flow-field calculation

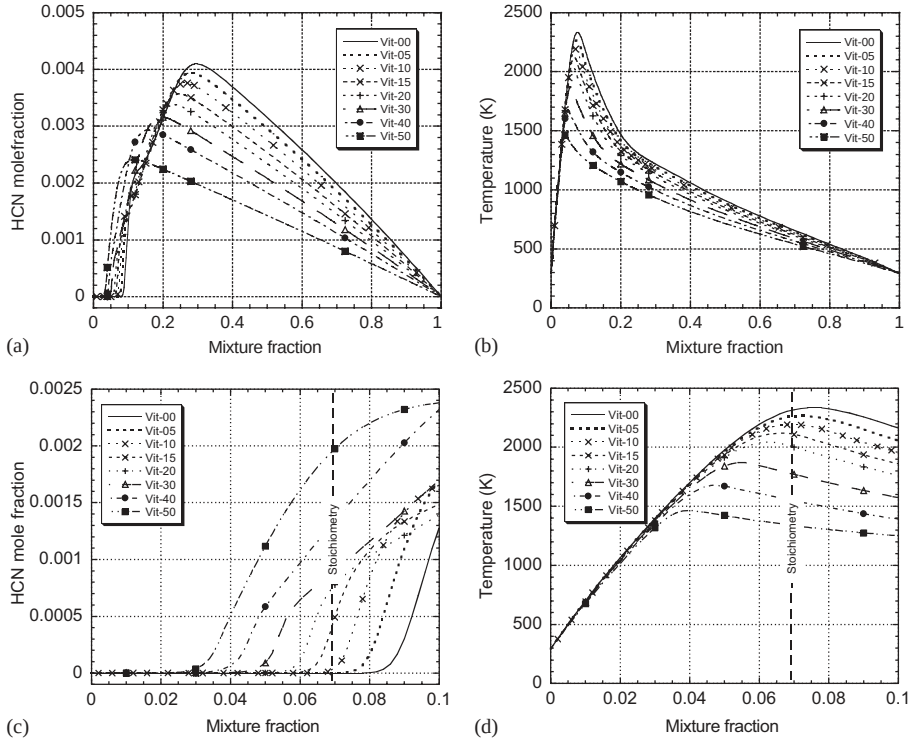

Fig. 3. Flamelet data for HCN and temperature with varying degrees of (cold) vitiation. No radiation losses.

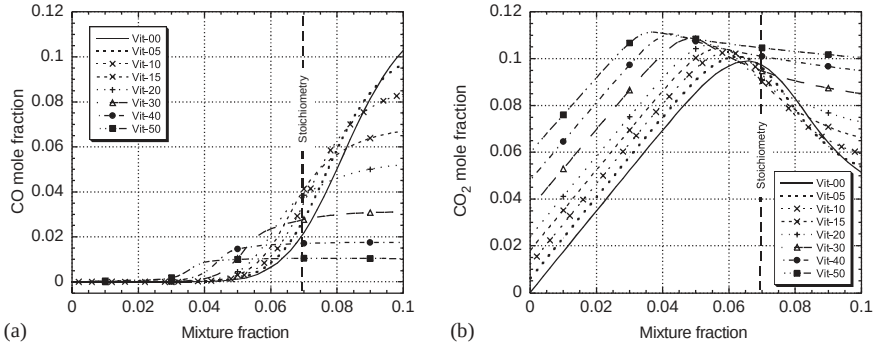

Fig. 4. Flamelet data for CO and CO_2 with varying degrees of (cold) vitiation. No radiation losses.

the flamelet options may be used either as adiabatic, constant radiation or an interpolation between flamelet sets of different radiation. Figs. 5(a–d) and 6(a–d) show the effects on the flamelet profiles of radiative heat losses.

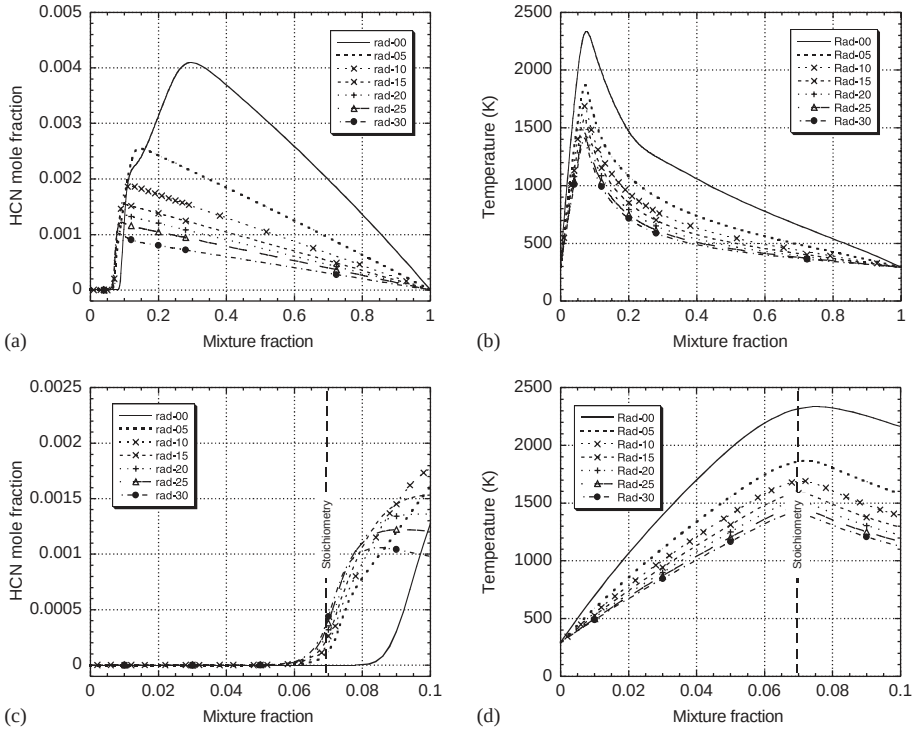

Fig. 5. Flamelet data for HCN and temperature with varying degrees of radiation losses. No vitiation.

The combustion temperature is lowered considerably by the radiative heat losses, as can be seen from Fig. 5(b). The mixture-fraction range around the stoichiometric condition is enlarged in Fig. 5(d) for the combustion temperature, and it is interesting to observe that a radiative loss of only 5% significantly lowers the combustion temperature. This has a distinct effect on the production of HCN, which is increased with radiative losses in the mixture-fraction range around stoichiometric conditions.

The combustion behaviour of carbon monoxide is complex. CO generally appears to decrease with an increase in radiative losses, see Fig. 6(a). However, at lower values of the mixture fraction on the lean side of stoichiometric conditions the opposite behaviour can be observed. From a very low mixture fraction up to approximately a mixture fraction of 0.03, the production of CO is enhanced with increasing radiation losses (Fig. 6(b)).

Carbon dioxide shows a similar, but reversed, behaviour. For values of the mixture fraction in the region of, and above, stoichiometric conditions, the mole fraction of CO_2 increases with increased radiative losses (Fig. 6(c)). For lower values of the mixture fraction, however, the mole fraction decreases with increased radiative losses (Fig. 6(d)).

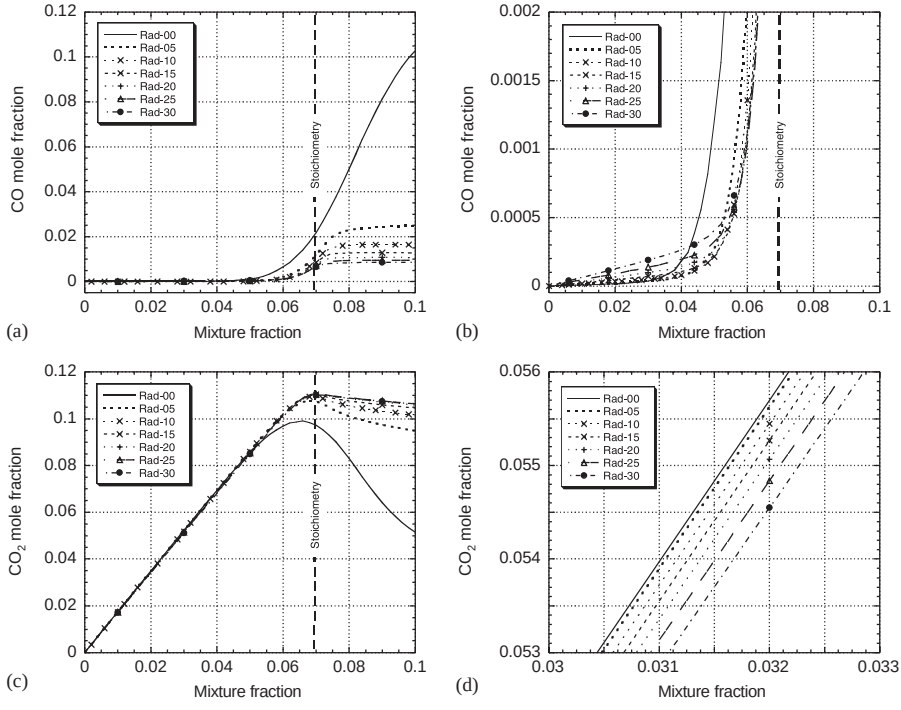

Fig. 6. Flamelet data for CO and CO_2 with varying degrees of radiation losses. No vitiation.

3. Experimental data

The experimental data used to investigate the capability of the model to predict the production of HCN was from a series of room-fires with pure nylon-6,6 fuel run in the TOXFIRE, EU-project at SP [15]. These tests focussed on an investigation of both the combustion conditions and combustion products. Gases, including CO and HCN, were measured continuously, and the combustion conditions were monitored by time-resolved measurements of the global equivalence ratio.

The fire tests were conducted in a room with dimensions according to the ISO 9705 room corner test. The room has one door opening of size 0.8×2.0 m (see Fig. 7) and changing the size of the door opening varied the ventilation rate to the fire between tests. The fire was placed on the floor on the room centreline at a distance $\frac{1}{3}$ of the room length from the back wall, where a fuel pan of size 1.44 m^2 (1.2×1.2 m^2) was loaded with nylon pellets.

Gas temperatures were measured using unshielded 0.5 mm type K thermocouples inside the room and in the door opening. Inside the room the thermocouples were placed on a vertical thermocouple tree 30 cm from the two walls in the front left-hand corner. In the opening, the thermocouples were placed on a smaller vertical tree 10 cm from the right-hand side of the opening (see Fig. 7).

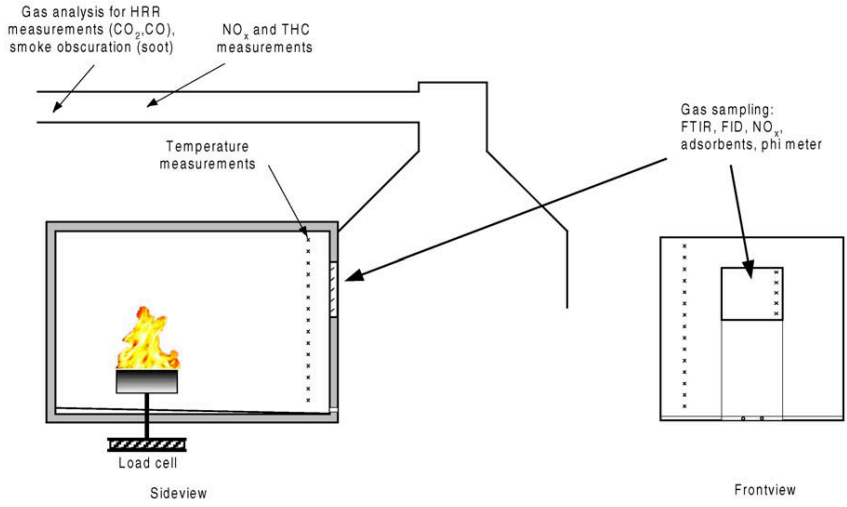

Fig. 7. The test arrangement used in the laboratory measurements [15].

The probe for the measurement of gas species and the probe for the measurement of the ϕ-value (the ϕ-value is a measure of the global equivalence ratio [16]) were placed diagonally from the top left-hand corner to the middle of the other side of the opening and varied in length depending on the size of the opening. Gas measurements of HCN, CO and other gases were obtained by FTIR technique [17]. The ϕ-value was measured using a specially constructed apparatus; more information on this apparatus is given in Ref. [16].

To reduce the door opening area, the lower part of the opening was blocked. For post-flashover (ventilation-controlled) compartment fires the inflow rate of air is given by

$$\dot{m} \approx 0.5A\sqrt{H}, \tag{1}$$

where A is the area of the opening in m^2 and H is the height of the opening in m. Tests with opening heights of 0.89 and 0.56 m were used for validation of the model.

The test with an opening height of 0.89 m gave a steady-state fuel mass flow of $20\,g\,s^{-1}$ corresponding to 500 kW after the initial fire growth period. The fire stayed rather constant at this burning level until the end of the experiment when the burning rate increased somewhat and the test was manually extinguished. The test with an opening height of 0.56 m yielded, as expected, initially a lower mass flow rate of fuel, about $15\,g\,s^{-1}$, corresponding to 350 kW heat release rate (HRR). This test had, however, a shorter steady-state period, after which the burning rate increased to reach a HRR of above 500 kW. This test reached flashover conditions before it was manually extinguished.

4. CFD simulations

4.1. Computational domain and design fires

The calculation domain included the test room described in the previous section and a region outside the room with the same length and width, and three times the height, of the room. The simulated walls were assumed to consist of lightweight concrete. The upper half of the walls and the ceiling were covered with a 5-cm layer of high-density mineral wool to avoid damage to the walls in the real tests. To simulate the same physical environment as closely as possible, the mineral wool covering was modelled similarly in the computer model. In the computer model, a fire source was placed in the room with area and position corresponding to the fire tests with nylon.

The nitrogen content of nylon is close to that of the model fuel (ethylene–methylamine, 3:1). However, the mass loss rate at a given heat release rate is about 30% less for the model fuel compared to nylon (i.e. the model fuel has a higher effective heat of combustion). As the level of HRR decides the demand of the oxygen in combustion, the same HRR, and thus the same degree of vitiation, as in the tests was assumed for the simulations. This implies that less fuel and thus less nitrogen was included in the simulated combustion compared to the real combustion of nylon. There have, however, been no attempts to correct the results presented in this paper for the lower mass flow rate of fuel in the simulations.

For the scenario with an opening height of 0.89 m, the rate of heat release was assumed to grow as αt^2, with $\alpha = 8.68\,\mathrm{W\,s^{-2}}$, up to value of 500 kW during a pre-burn time period (first four minutes), after which the HRR was held constant at that level. This t^2-approximation was chosen to facilitate the computation of the initial flow-field, i.e. to achieve a converged solution at each time-step more quickly. Similarly, for the scenario with an opening height of 0.56 m, the HRR was assumed to grow as αt^2 with time up to 350 kW.

The computational domain was divided into 233 100 small control volumes ($42 \times 75 \times 74$ in x-, y- and z- directions, respectively). This corresponds to an average cell size of about 10 cm (in all three directions). The finest resolution was used in the combustion region, where the largest gradients in field parameters are expected. In the fire plume and the near vicinity, a typical cell size between 2 and 5 cm was used. The space was divided finely in the vertical direction (y-coordinate) in particular, to be able to resolve the chemistry in the plume flow. In the other regions inside the room, a typical cell size of 10 cm, and outside the room 15 to 25 cm, was used.

4.2. Computational details

The simulations were made using the transient mode of SOFIE. The length of the time step was chosen depending on the actual situation occurring during the fire history. In the beginning and during most of the simulation time, a time step of one second was used. Approaching a vitiated situation the time step was shortened. In the most vitiated situation, i.e. when using the smallest opening, a time step as short

as 0.25 s was necessary to establish a converged solution. The convergence of the solution was controlled keeping the normalised residuals of all solved variables as low as possible, usually below 0.001. The under-relaxation parameter for momentum was set to 0.12 (in all three directions) at the beginning of the simulation and was reduced further to about half the original value later in simulation, to avoid oscillating behaviour in solution.

Simulations were run both with the non-vitiated and the cold vitiated flamelet options. In all cases, the interpolated radiative loss flamelet-option was used. The discrete transfer radiation model (DTRM) assuming 16 rays (default value) was used in the simulations. It was not feasible to use a higher number of rays in these simulations, because the fine grid in the fire room reserved so much computer memory that the computations could not have been performed in a reasonable time. No soot model was used and hence the radiative losses from soot were not included.

The following cases were run:

Case 1A: No vitiation, opening height 0.89 m.
Case 1B: Vitiation (cold), opening height 0.89 m.
Case 2: Vitiation (cold), opening height 0.56 m.

In vitiated cases the degree of vitiation was manually changed based on the oxygen contents of the air entrained to the fire. The first 160 s in Case 1B were run as non-vitiated. At 160 s, the vitiation fraction 0.05 was chosen. At 180 s, the vitiation fraction was increased to 0.15, at 200 s to 0.20 and after 240 s (i.e., the time the simulation reached a steady-state HRR of 500 kW) the vitiation fraction was held at 0.30. In Case 2 the vitiation fraction was increased more rapidly, so that the vitiation fraction of 0.30 was reached at 180 s. The actual vitiation increased to near the 0.40 level after 240 s (i.e., the time for reaching a steady-state HRR; in this case 350 kW), but the low oxygen content (12.6%) in the air using this vitiation level resulted in a non-converged solution. This low oxygen concentration was not able to sustain combustion in the computer model, despite knowledge to the contrary from the experimental data. Thus, the vitiation fraction 0.30 was used during the rest of this simulation.

The global equivalence ratio was calculated by comparing the ratio of the mass flow of fuel from the fire source to the mass flow of oxygen through the door with the stoichiometric relation of fuel and oxygen

$$\Phi = \frac{Y_{\mathrm{F,in}}/Y_{\mathrm{O_2,in}}}{(Y_{\mathrm{F}}/Y_{\mathrm{O_2}})_{\mathrm{st}}}, \tag{2}$$

where $Y_{\mathrm{F,in}}$ is the mass flow of fuel from the fire source, $Y_{\mathrm{O_2,in}}$ is the oxygen mass flow into the room through the opening and $(Y_{\mathrm{F}}/Y_{\mathrm{O_2}})_{\mathrm{st}}$ is the stoichiometric fuel to oxygen ratio. This method is valid assuming a nearly steady-state fire in relation to the length of the overall flow time of gases through the room.

5. Results and discussion

Table 1 summarises the calculated gas temperatures for the two simulations of the room fire scenario with the 0.89 m opening (Cases 1A and 1B) and compares these with measured values. Table 2 similarly shows the results for the single simulation of the room fire scenario with the 0.56 m opening (Case 2). In all cases T_1, T_2 and T_3 are temperatures at heights 2, 1.4, and 0.95 m in the front left-hand corner of the room, respectively. $T_{opening}$ is the temperature of gas flowing out of the door opening, 10 cm below the soffit for the room scenario with the larger opening, and 8 cm below the soffit for the room scenario with the smaller opening. Correction calculations for the thermocouple temperatures were made. These showed, however, no noticeable errors (maximum error approximately 20 K) in the recorded temperatures located both inside the room and in the opening.

The results are compared after the so-called pre-burn period, when the HRR has been stabilised at a constant level. In the computer simulations that pre-burn time was 4 min during which the HRR increased as t^2. In the tests, the pre-burn time was longer and the HRR history more complicated due to the ignition behaviour of the fuel.

Table 1
Calculated values of gas temperatures (°C) for simulations with non-vitiated flamelets (Case 1A) and for simulations with vitiated flamelets (Case 1B) compared with measured values

Time (min) after pre-burn	Calculation					Measurement			
	Flamelet option	T_1	T_2	T_3	$T_{opening}$	T_1	T_2	T_3	$T_{opening}$
1	Non-vitiated	578	541	468	553	695	649	550	557
	Vitiated	621	582	501	555				
2	Non-vitiated	582	547	474	564	716	670	575	567
	Vitiated	622	582	501	558				

Room fire scenario: opening height 0.89 m.

Table 2
Calculated values of gas temperatures (°C) using vitiated flamelet option compared with measured values

Time (min) after pre-burn	Calculated				Measured			
	T_1	T_2	T_3	$T_{opening}$	T_1	T_2	T_3	$T_{opening}$
1	590	545	469	525	626	593	535	536
2	605	549	467	525	667	631	563	559

Room fire scenario: opening height 0.56 m (Case 2).

In the non-vitiated calculation of the room fire scenario with the 0.89 m opening, the calculated gas temperatures in the corner location are between 80 and 130 K lower than the measured temperatures. In the corresponding vitiated calculation, these temperatures are still lower, but somewhat closer to the measured values; the discrepancy is between 50 and 90 K. At the opening, the difference between the measured and calculated temperature is negligible, less than 10 K in both vitiated and non-vitiated cases.

The scenario with the smaller opening was simulated using vitiation only, as this option gave the best results for the larger opening. Once again the calculated temperatures inside the room are lower than those measured (see Table 2). The temperature discrepancy is of the same order as in the vitiated case for the larger opening. The simulated temperatures in the opening again agree well with the measured temperatures.

Preparatory calculations showed that a cell size of 2 cm in the fire region was necessary to obtain reasonable resolution of gas species. However, chemical reactions also occur in other regions in the compartment such as in the hot gas layer. In this study, however, somewhat larger cells were used in the hot gas layer region. This may have influenced the results if some of the combustion has in reality been occurring here. This could be one explanation of the somewhat lower temperatures in the gas layer.

The main species concentrations and the global equivalence ratio, Φ, for the room fire scenario with the larger opening (Cases 1A and 1B) are summarised in Table 3. Comparison of the global equivalence ratio calculated from the simulations with that from the measurements would be one way to make an assessment of whether the simulated combustion conditions were relevant to those in the real fire. As was seen from the investigation of the flamelet profiles including vitiation (Figs. 3 and 4) the production of both HCN and CO is very sensitive to the prevailing fuel/oxygen ratio. An error in the simulation regarding available oxygen for the combustion would thus result in a large error for gas species.

Table 3
Calculated species concentrations and global equivalence ratio in the opening for calculations with non-vitiated flamelets (Case 1A) and for calculations with vitiated flamelets (Case 1B) compared with measured values

Time (min) after pre-burn	Calculation					Measurement			
	Flamelet option	HCN (ppm)	CO (ppm)	CO_2 (%)	Φ	HCN (ppm)	CO (ppm)	CO_2 (%)	Φ
1	Non-vitiated	3	210	5.3	0.43	36	450	4.2	0.55
	Vitiated	23	630	4.5	0.52				
2	Non-vitiated	3	220	5.4	0.43	35	460	4.2	0.55
	Vitiated	27	740	5.5	0.65				

Room fire scenario: opening height 0.89 m.

In the non-vitiated simulation, the equivalence ratio is stabilised at 0.43, 1 min after the pre-burn time. This underestimates the measured value by about 20%. In the vitiated calculation the equivalence ratio initially is 0.52. This is very close to the measured value of the equivalence ratio. However, this simulation did not show stable combustion conditions during the investigated time period. After 2 min the calculated value increased to 0.65 (overestimating the experimental value by nearly 20%).

Both calculated HCN and CO concentrations are much lower than measured values when the non-vitiated flamelet option is used. As was seen from the equivalence ratio, the simulated combustion conditions were on the well-ventilated side compared to those prevailing in the experiments, which can explain the under-prediction in HCN and CO concentrations and also the over-prediction of CO_2. This indicates that the vitiated flamelet option would be the valid one in this case.

In the vitiated calculation, the HCN levels are about 7–8 times higher than in the non-vitiated calculation. After 1 min, the calculated global equivalence ratio in this case is close to that from the measurement and the predicted concentration of HCN is of the same order of magnitude as the measured values. Similarly, the calculated CO concentrations increased significantly using the vitiated scenario. For CO, the calculated results with the vitiated flamelet option were over-predicted, although they were of the same order of magnitude as measured values. One would expect the concentrations of CO_2 to be reduced using the vitiated flamelet option, as this generally would reduce the combustion efficiency. This is also the case for the simulation results after 1 min where the vitiated calculation gives a lower CO_2 concentration, which actually is very close to the measured value. However, after 2 min, the predicted CO_2 from the vitiated calculation rises significantly. This behaviour was not seen from the measurements and is difficult to explain, especially as the calculated equivalence ratio is increased. Generally, however, of the two flamelet options the best agreement with measurement is with the vitiated option, see Table 3.

When reducing the opening size, the measured concentrations of HCN are increased strongly (cf. Table 4). The vitiation of the air in the room increases faster in the case with the smaller opening (Case 2), which is reflected in the higher ϕ-values measured. The higher vitiation lowers the flame temperature and thus influences the

Table 4
Calculated species concentrations and global equivalence ratio in the opening for calculations with vitiated flamelets compared with measured values

Time (min) after pre-burn	Calculated				Measured			
	HCN (ppm)	CO (ppm)	CO_2 (%)	Φ	HCN (ppm)	CO (ppm)	CO_2 (%)	Φ
1	380	3600	8.3	0.94	220	790	8.6	0.70
2	430	3600	8.4	0.94	220	780	8.4	0.75

Room fire scenario: opening height 0.56 m (Case 2).

gas chemistry and causes a significantly higher production of HCN (see e.g. Fig. 3(c)). Similarly, the CO concentrations are higher in the scenario with the smaller opening. This trend is also seen from the simulation (see Table 4), but the increase for the calculated values is stronger, and HCN, and particularly CO, are over-predicted compared to the measurements. The calculated global equivalence ratio is, however, about 30% higher than the measured ratio.

A contributing factor for the higher global equivalence ratios attained in the simulations, compared to the measurements in the opening during the experiments, is that the air entraining through the opening in the simulations is vitiated, i.e. a single value of vitiation is assumed for the entire computational domain. This is not the case in a real vitiated room-fire, where the fresh air from the opening is mixed with combustion products (i.e. vitiated) before reacting with the fuel.

The fast chemistry approach that has been assumed in this work is possibly not the best approach for describing the formation of species with slower kinetics, such as NO_X and soot. The faster the chemistry, the more valid is the stationary laminar flamelet concept that was used in this study. As one route of the HCN formation is via NO_X, the fast chemistry approach might not be entirely correct in describing the HCN kinetics. This might thus affect the calculated concentrations of HCN in this study. For calculation of slow kinetics, the flamelet model could possibly in the future be modified to take account of the residence time of species.

6. Conclusions

In the work presented here, a kinetic scheme of the conversion of a nitrogen-containing model fuel (a mixture of methylamine and ethylene) to combustion products has been applied. The simulations discussed in this paper were, however, of fire tests with nylon as a fuel. To quantitatively compare the results of the experiments with those of the simulation, one has to make the presumption that the pyrolysis chemistry of nylon gives the same types and proportions of nitrogen-containing breakdown products as those described by the reaction mechanism for methylamine. The results of the simulations indicate however that this approach has some success.

Important results from the study are:

- The results from the simulations show that the present flamelet model is able to semi-quantitatively predict the production of HCN in a room fire.
- Both the production during well-ventilated conditions, and the increased production during under-ventilated conditions were captured by the model.
- Similarly, for CO, the model semi-quantitatively predicted the production from a room fire, although the simulation of CO seamed to be more prone to over-predictions at vitiated conditions.

The simulations presented with the model should, however, be regarded as an initial test only of the model's capability to simulate the gas-phase chemistry of fires with an arbitrary nitrogen-containing fuel.

There are, however, some obvious weaknesses of the present application of the model:

- The model-fuel is based on the chemistry of gas-phase methylamine mixed with ethylene, and does not describe the pyrolysis and subsequent gas-phase reactions of nylon.
- Further, the mass-loss rate of the model-fuel in the simulations was lower compared to the actual mass-loss of nylon in the experiments. This was necessary to achieve the same total HRR from the fuel in the simulation as in the experiments.
- The flamelet model assumes fast chemistry and therefore describes the flaming region best. As such, it is important to model the flame region carefully. Generally, the flamelet model needs a finer mesh compared to the other more commonly used combustion model, the eddy break-up model, in order to resolve the chemical species formation in space and time.

The results of this work show that there is large difference in the calculated species concentrations when using different flamelet options. The non-vitiated case produced lower concentrations of both CO and HCN, compared to vitiated case. In particular, the HCN concentration was nearly 10 times lower. The vitiated option proved to be more consistent relative to the measurements. Hence, when simulating a certain scenario, one should take into account whether the air in the entrainment region to the fire is vitiated or not.

Although this study shows some weaknesses in the application of the model-fuel for a solid fuel and further in some assumptions of the model, the results of the simulations are encouraging, proving that the model is capable of semi-quantitative prediction and suggesting that the modelling approach should be validated further for other scenarios and fuels.

Acknowledgements

This project was sponsored by the Swedish Fire Research Board (BRANDFORSK), which is gratefully acknowledged. The authors would also like to express appreciation to Dr. Fabian Mauss at the Division of Combustion Physics, Lund University and to Prof. Göran Holmstedt at the Department of Fire Safety Engineering, Lund University, for comments and valuable discussion during the project.

References

[1] Simonson, M, Tuovinen, H, Emanuelsson, V. Formation of hydrogen cyanide in fires—a literature and experimental investigation. SP REPORT 2000:27.
[2] Fenimore CD. J Combust Flame 1972;19:289.
[3] Bowman CT. In: Bartok W, Sarofim AF editors. Fossil fuel combustion—a source book. New York: Wiley; 1991. p. 314.

[4] Miller JA, Bowman CT. Prog Energ Combust Sci 1989;15:287.
[5] Cox G. Combustion fundamentals of fire. London: Academic Press; 1995.
[6] Tuovinen H. Application of flamelet chemistry model to vitiated methane–air diffusion flames. Report LUTVDG/TVBB3065-SE, 1992, Department of Fire Safety Engineering, Lund University.
[7] Tuovinen H. Modelling of laminar diffusion flames in vitiated environment. Fourth international symposium on fire safety science, 13–17 June 1994, Ottawa, Canada.
[8] Tuovinen H, Blomqvist P. Modelling of hydrogen cyanide formation in room fires. SP REPORT 2003:10, ISBN 91-7848-941-5, 2003.
[9] Hoyermann K, Mauss F, Zeuch T. A detailed chemical reaction mechanism for the oxidation of hydrocarbons and its application to the analysis of benzene formation in fuel rich premixed laminar acetylene and propene flames, Phys Chem Chem Phys, 2004.
[10] Klaus P, Warnatz JA. Further contribution towards a complete mechanism for the formation of NO in flames. VDI Berichte Nr. 1313, Verein Deutscher Ingenieure, Germany, 1997.
[11] Klaus P, Entwicklung eines Detailierten Reaktionsmechanismus zur Modellierung der Bildung von Stickoxiden in Flammenfronten, PhD thesis, Universtät Heidelberg, 1997.
[12] Balthasar M. Detailed soot modelling in laminar and turbulent reacting flows. Doctoral dissertation, Lund Institute of Technology, Department of Combustion Physics, ISBN 91-628-4356-7, 2000.
[13] Kantak MV, De Manrique KS, Aglave RH, Hesketh RP. Methylamine oxidation in a flow reactor: mechanism and modelling. Combust Flame 1997;108:235–65.
[14] Welch S, Rubini P. SOFIE—simulation of fires in enclosures, users guide. Cranfield, UK: Cranfield University; 1996.
[15] Lönnermark A, Blomqvist P, Månsson M, Persson H. TOXFIRE—fire characteristics and smoke gas analysis in under-ventilated large-scale combustion experiments, tests in the ISO 9705 room. SP-REPORT 1996:45.
[16] Lönnermark A, Babrauskas V. TOXFIRE—fire characteristics and smoke gas analysis in under-ventilated large-scale combustion experiments, theoretical background and calculations. SP-REPORT 1996:49.
[17] Blomqvist P, Lindberg P, Månsson M. TOXFIRE—fire characteristics and smoke gas analysis in under-ventilated large-scale combustion experiments, FTIR measurements. SP-REPORT 1996:47.